

Title: Maximizing the impact of limited vaccine supply under different epidemic conditions: a two-city monkeypox modelling analysis

Authors: Jesse Knight^{1,2} and Sharmistha Mishra^{1,2,3,4}

¹MAP Centre for Urban Health Solutions, Unity Health Toronto

²Institute of Medical Science, University of Toronto

³Institute of Health Policy, Management, and Evaluation, University of Toronto

⁴Division of Infectious Diseases, Department of Medicine, University of Toronto

Journal: (preprint)

Date: 2022 Aug 15 (draft)

Abstract

TODO

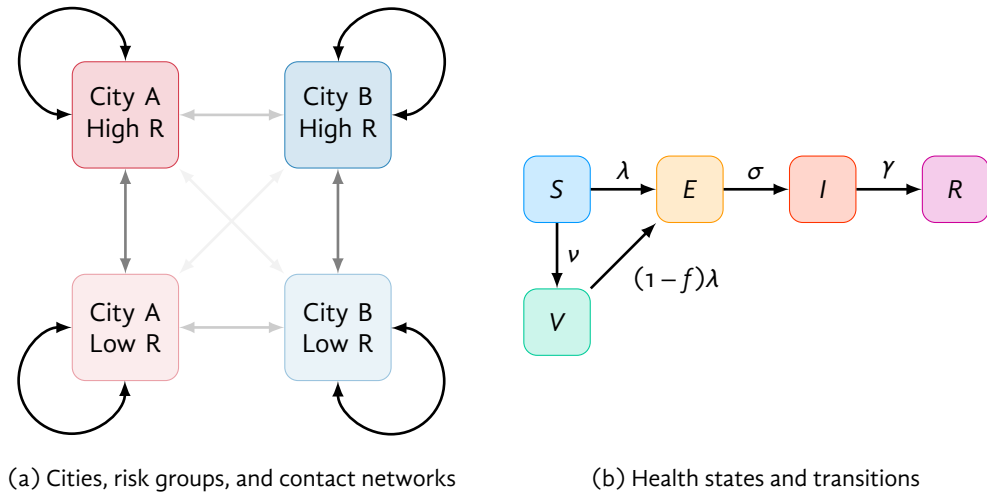


Figure 1: Model structure

(a) High/Low R: risk groups; arrow opacity is proportional to contact network connectivity between groups. (b) S: susceptible; V: vaccinated; E: exposed; I: infectious; R: recovered. See Table A.1 and Appendix A for rate definitions.

1 Introduction

...

We sought to explore optimal allocation of a fixed supply of monkeypox vaccine across two cities — i.e. weakly connected transmission networks — under different epidemic conditions. Specifically, we explored differences between cities in: population size; epidemic potential (R_0); imported/seed cases; and connectedness of the cities. The transmission network explored was loosely representative of Ontario gay, bisexual, and other men who have sex with men (GBMSM), reflecting the Ontario population with highest monkeypox burden at present. However, our aim was not to precisely model specific Ontario cities, but to produce generalizable insights into efficient vaccine prioritization.

2 Methods

We constructed a deterministic compartmental SVEIR (susceptible, vaccinated, exposed, infectious, recovered) model of monkeypox transmission. The modelled population aimed to represent the Ontario GBMSM community, and included two levels of sexual risk (higher, lower) and two weakly connected transmission networks (cities A, B). Figure 1a illustrates the modelled city/risk strata, Figure 1b illustrates the SVEIR health states, and Table 1 summarizes the default model parameters.

We initialized all model runs with 10 imported/seed cases, distributed across the exposed and infectious stages proportionally by mean stage duration. We then simulated distribution of 5000 vaccine doses over 15 days from day 60, doses that were imperfectly prioritized to

Table 1: Model parameters, including default values and ranges explored via grid sweep

Parameter	Stratum	Value	Range	Ref
Population size	overall	100,000		
Fraction higher risk	fraction in city A	.50	[.20, .80]	
	city A	.10	[.01, .50] ^a	
	city B	.10		
Contact rate	non-sexual, everybody	1		
	sexual, low risk	.01		
	sexual, high risk, city A	.178 ^b	[.10, .25] ^a	
	sexual, high risk, city B	.178 ^b		
Assortativity	cities, all contacts	.90	[.70, 1.0]	
	risk, non-sexual	0		
	risk, sexual	.50		
Per-contact SAR	non-sexual	.05		
	sexual	.90		
Initial infections	overall	10		
	fraction in city A	.50	[0.0, 1.0]	
Duration of period	latent/incubation	7		
	infectious/symptoms	21		
Fraction isolated among infected		.50		
Vaccines available		5000		
Vaccine effectiveness		.85		
Vaccine prioritization sensitivity	high risk	.90		
Vaccine allocation	city A	.50	[0.0, 1.0] ^c	

All durations in days; all rates in per-day. SAR: secondary attack rate. ^a Calculated to fit $R_0 \in [1, 2]$. ^b Calculated to fit $R_0 = 1.5$. ^c Optimized parameter.

the higher risk group with 90% sensitivity — i.e. 4500 doses reach the higher risk group and 500 each the low risk group.

Using this model, we explored optimal vaccine allocation between cities A and B over a range of epidemic conditions. For a given set of conditions, we defined the optimal vaccine allocation as that which resulted in the fewest cumulative infections by day 120 in both cities.

We chose this 60-day time horizon and fixed 5000 vaccine doses to reflect a plausible medium-term optimization problem relevant to the early monkeypox situation in Ontario. In reality, multiple changing time horizons may require consideration, different numbers of doses may become available, and different rates of vaccination may be possible. We aimed to obtain generalizable insights about the relationships between specific epidemic conditions and efficient geographic prioritization of vaccines during an outbreak.

As one specific example setting, we chose parameters representative of Toronto (city A) and another medium-sized Ontario city (city B). Based on ... 80,000 and 20,000 GBMSM population size, respectively. ... 10% sexual network connectivity ($\epsilon_c = 0.9$). ... $R_0 = 2.0$ in Toronto versus 1.5 in city B. ... 100% imported/seed cases in Toronto. ... We then compared

two strategies of vaccine allocation by city: (a) proportional to population size; (b) fewest infections by day 120.

Additionally we performed a “grid sweep” of the following epidemic conditions, and identified the optimal vaccine allocation between cities A and B for each combination of conditions:

- relative size of city A versus B ($1/4$ to 4 times)
- relative epidemic potential in city A (R_0 in city A from 1 to 2, versus fixed 1.5 in city B),¹ adjusted via the sexual activity of the higher risk group in the city A
- between-city mixing (0 to 30% of all contacts formed randomly between cities)
- fraction of imported/seed cases in city A versus B (0–100%)

3 Results

Figure 2 illustrates modelled monkeypox incidence and cumulative infections in “Toronto” versus city B under different vaccine allocation strategies. Due to the larger population size, greater epidemic potential (R_0), and having all imported/seed cases in Toronto in this scenario, allocating all 5000 vaccine doses to Toronto yielded the fewest infections by day 120: 1630 (c). Allocating vaccines proportionally to city size (b) yielded 1956 infections, while no vaccination (a) yielded 3466 infections.

As shown in Figure 2c, allocating most/all doses to one city (A) allows incidence to rise exponentially in the other city (B). However, this approach can still avert more infections overall over shorter time horizons, after which more doses may become available. Figure ?? illustrates the opposite case (default model parameters in Table 1): two identical cities with equal seeding, where the optimal allocation is equal between cities.

Figure 3 illustrates optimal vaccine allocation between cities A and B across different epidemic conditions. Figures ??–?? further illustrate the absolute and relative numbers of infections averted under optimal allocation versus no vaccination (??–??), and versus vaccine allocation proportional to city size (??–??). Thus, Figures ??–?? show under what conditions optimal allocation is most important.

The strongest determinants of optimal vaccine allocation were: relative epidemic potential (R_0), share of seed cases, and city size; though city size was proportional to the size of the higher risk group under our modelling assumptions. Thus, if a larger city had large R_0 and the majority of seed cases, it was best to allocate most/all doses to that city in our analysis (solid red/blue corners in Figure 3).

For smaller cities with large R_0 and the majority of seed cases, it was sometimes possible to vaccinate the entire higher risk group; in this case, the remaining doses were best allocated to the other city, yielding the plateaus (solid-colour triangles) in Figure 3: (a,d,g) upper right; (c,f,i) lower left. This plateau highlights how priority populations can change if/after high levels of coverage are achieved in other populations.

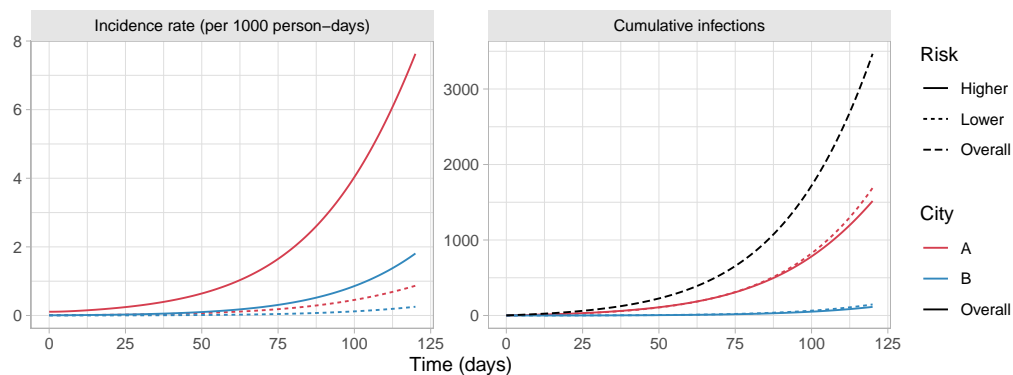
¹City-specific R_0 calculated assuming no inter-city mixing.

When cities with most/all seed cases had smaller R_0 , optimal allocation saw doses shared between cities (to varying degrees), suggesting that both risk-based (reflecting R_0) and proximity-based (reflecting initial cases) prioritization strategies worked together to minimize transmission. In such cases, the other city necessarily had few/no seed cases but larger R_0 , to which the same findings apply. These conditions are represented by the yellow diagonal segments in all facets of Figure 3.

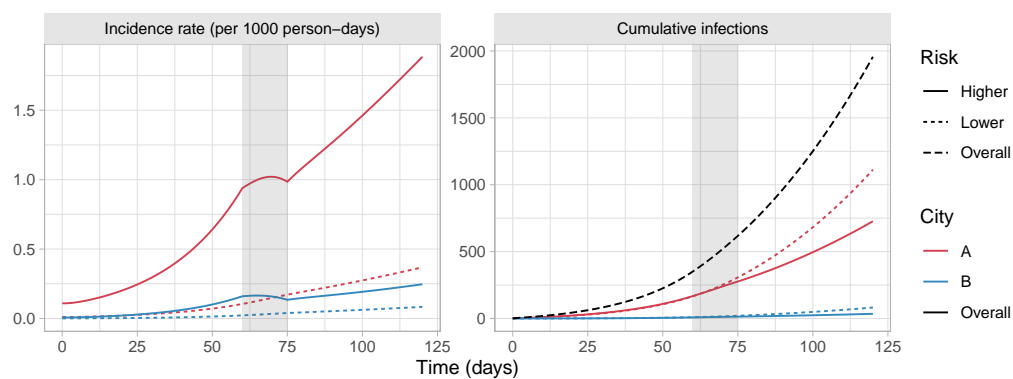
Finally, increased levels of mixing between cities mainly acted to reduce the influence of initial seed cases, and increase the influence of R_0 on optimal allocation of vaccines to each city; this finding is visible in Figure 3 as stronger vertical gradients (contours are more horizontal) in (a,b,c) with more inter-city mixing, versus stronger horizontal gradients (contours are more vertical) in (g,h,i) with less inter-city mixing.

4 Discussion

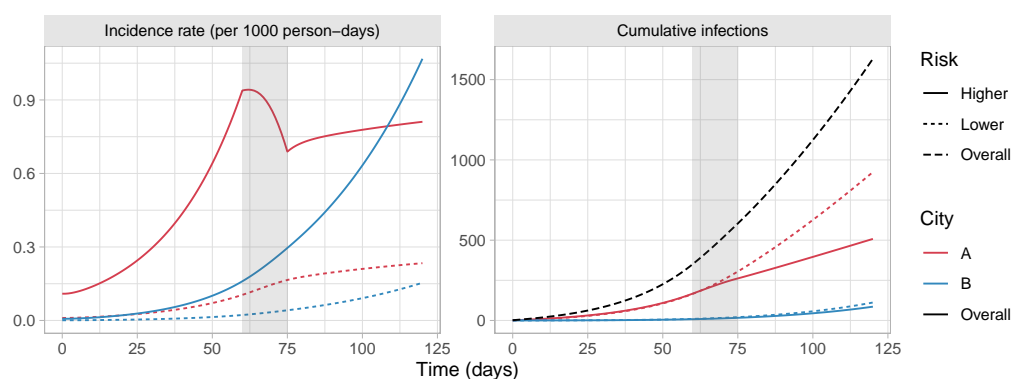
We sought to explore how different epidemic conditions could affect optimal allocation of a fixed supply of monkeypox vaccine across two weakly connected transmission networks (e.g. cities). Under our modelling assumptions, we found that vaccines could generally avert more infections when prioritized to a larger city, a city with more initial infections, and a city with greater epidemic potential R_0 defined by contact rates in a higher risk group.



(a) No vaccination



(b) Proportional to city size: 75% city A, and 25% city B



(c) Optimal (most infections averted by day 120): 100% city A

Figure 2: Modelled monkeypox incidence and cumulative infections in two cities under two different vaccine allocation scenarios

Gray bar indicates period of vaccine roll-out (days 60–75). Cities loosely reflect Toronto and another medium-sized Ontario city.

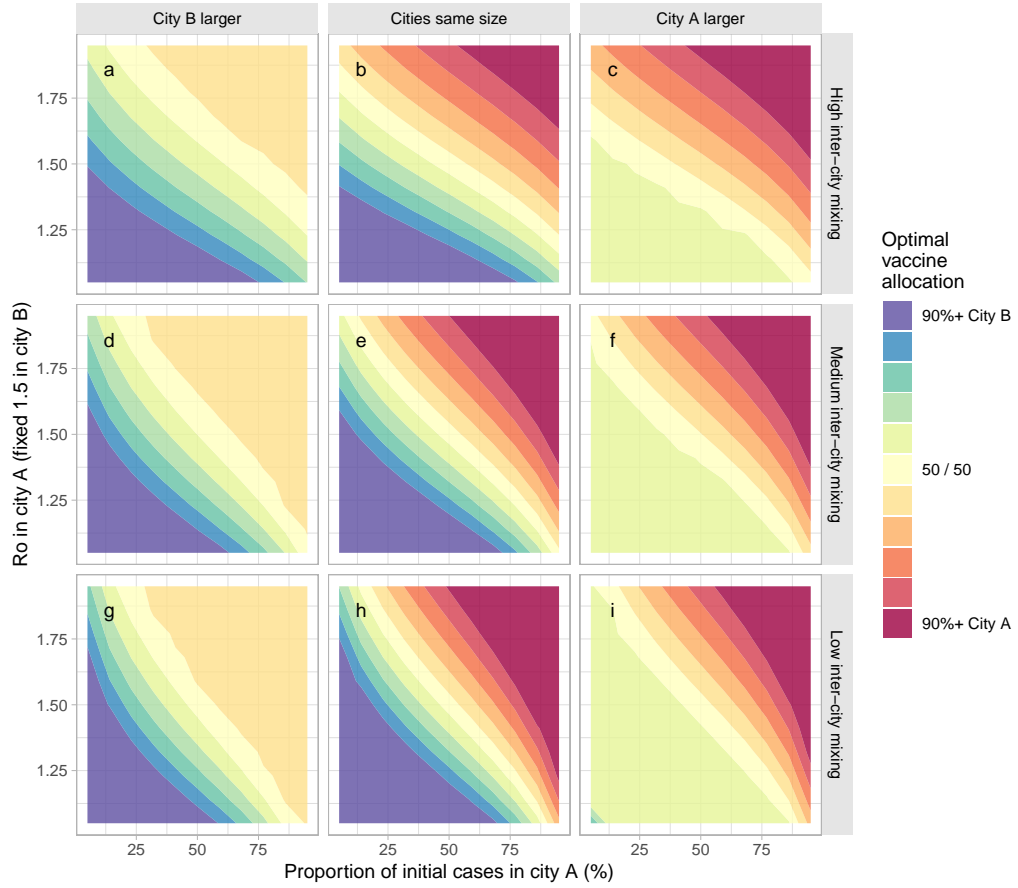


Figure 3: Optimal vaccine allocation between two cities under different epidemic conditions

R_0 in city A varies via the sexual activity among the high risk group in city A. Optimal allocation is defined as fewest cumulative infections by day 120. Larger city is 3 times the size of the other city. Most, moderate, and least inter-city mixing use $\epsilon_c = \{0.8, 0.9, 0.95\}$, respectively.

References

- [1] Public Health Ontario. *Monkeypox in Ontario: May 20, 2022 to June 20, 2022*. June 2022.

Funding

The study was supported by: the Natural Sciences and Engineering Research Council of Canada (NSERC CGS-D); and the University of Toronto Emerging and Pandemic Infections Consortium (EPIC) MPXV Collaborative Rapid Research Response.

Acknowledgements

We thank: Kristy Yiu (Unity Health Toronto) for research coordination support; Huiting Ma, Linwei Wang, Oliver Gatalo, and Ekta Mishra (Unity Health Toronto) for support conceptualizing and parameterizing the model.

Contributions

JK and SM conceptualized and designed the study, and drafted the manuscript. JK developed the model, conducted the analyses, and generated the results. DT reviewed the results and contributed to manuscript writing.

Data Availability

All analysis code is available at: github.com/mishra-lab/mpox-model-compartmental

APPENDIX

Title: Maximizing the impact of limited vaccine supply under different epidemic conditions: a two-city monkeypox modelling analysis

Authors: Jesse Knight^{1,2} and Sharmistha Mishra^{1,2,3,4}

¹MAP Centre for Urban Health Solutions, Unity Health Toronto

²Institute of Medical Science, University of Toronto

³Institute of Health Policy, Management, and Evaluation, University of Toronto

⁴Division of Infectious Diseases, Department of Medicine, University of Toronto

Date: 2022 Aug 15 (draft)

A Model Details

Table A.1 summarizes the notation used.

Table A.1: Notation

Symbol	Definition
c	city index $\in \{A, B\}$
r	risk group index $\in \{\text{high, low}\}$
y	type of contact index $\in \{\text{sexual, non-sexual}\}$
N	population size
C	contact rate
Q	total contacts offered: NC
ϵ	assortativity parameter $\in [1: \text{assortative, } 0: \text{random}]$
λ	incidence rate (force of infection)
β	transmission probability
σ^{-1}	duration of latent/incubation period
γ^{-1}	duration of infectious/symptom period
Φ	probability of contact formation
ρ	proportion isolating among infectious
ν	vaccination rate
f	vaccine effectiveness

A.1 Differential Equations

Equation (A.1) summarizes the system of differential equations for the SVEIR health states; each equation is repeated for each combination of city c (A, B) and risk group r (high, low) (4 total), but we omit the cr index notation for clarity.

$$\frac{d}{dt}S = -\nu S - \lambda S \quad (\text{A.1a})$$

$$\frac{d}{dt}V = +\nu S - (1-f)\lambda V \quad (\text{A.1b})$$

$$\frac{d}{dt}E = +\lambda S + (1-f)\lambda V - \sigma E \quad (\text{A.1c})$$

$$\frac{d}{dt}I = +\sigma E - \gamma I \quad (\text{A.1d})$$

$$\frac{d}{dt}R = +\gamma I \quad (\text{A.1e})$$

A.2 Incidence Rate

The incidence rate (force of infection) for non-vaccinated susceptible individuals in city c and risk group r ("group cr ") is defined as:

$$\lambda_{cr} = \sum_{y c' r'} (1 - \rho) \beta_y C_{y cr} \Phi_{y cr c' r'} \frac{I_{c' r'}}{N_{c' r'}} \quad (\text{A.2})$$

where: ρ is the proportion isolating among infectious; β_y is the transmission probability per type- y contact; $C_{y cr}$ is the type- y contact rate among group cr ; $\Phi_{y cr c' r'}$ is the probability of type- y contact formation with group $c' r'$ among group cr ; and $N_{c' r'}$ is the size of group $c' r'$.

Among vaccinated, the incidence rate is simply reduced by a factor $(1 - f)$, where f is the vaccine effectiveness (take-type).

A.3 Mixing

Mixing between risk groups and cities was implemented using an adaptation of a common approach [1, 2]. We denote the total contacts "offered" by group cr as: $Q_{cr} = N_{cr} C_{cr}$; and denote the margins $Q_c = \sum_r Q_{cr}$; $Q_r = \sum_c Q_{cr}$; and $Q = \sum_{cr} Q_{cr}$. The probability of contact formation with group $c' r'$ among group cr is defined as:

$$\Phi_{cr c' r'} = \epsilon_c \delta_{cc'} \left(\epsilon_r \delta_{rr'} + (1 - \epsilon_r) \frac{Q_{c' r'}}{Q_{c'}} \right) + (1 - \epsilon_c) \frac{Q_{c'}}{Q} \left(\epsilon_r \delta_{rr'} + (1 - \epsilon_r) \frac{Q_{r'}}{Q} \right) \quad (\text{A.3})$$

where: $\delta_{ii'} = \{1 \text{ if } i = i'; 0 \text{ if } i \neq i'\}$ is an identity matrix; and $\epsilon_c, \epsilon_r \in [0, 1]$ are assortativity parameters for mixing among cities and risk groups, respectively, such that $\epsilon = 1$ yields complete group separation and $\epsilon = 0$ yields completely random (proportionate) mixing. For clarity, we omit the index of contact type y , although ϵ_r, C_{cr} and thus $\Phi_{cr c' r'}$ are all further stratified by y .

A.4 City R_0

The basic reproduction number R_0 for each city was defined in the absence of vaccination and ignoring between-city mixing — i.e. with $\epsilon_c = 1$. Following [3], we define R_0 as the dominant eigenvalue of the city-specific next generation matrix K ; matrix elements $K_{rr'}$ are defined as:

$$K_{rr'} = (1 - \rho) \sum_y \beta_y C_{y r} \Phi_{y r r'} \frac{N_r}{N_{r'}} \gamma^{-1} \quad (\text{A.4})$$

where: ρ is the proportion isolating among infectious; β_y is the transmission probability per type- y contact; $C_{y r}$ is the type- y contact rate among group r ; $\Phi_{y r r'}$ is the probability of type- y contact formation with group r' among group r ; N_r is the size of group r ; and γ^{-1} is the duration of infectiousness.

A.5 Vaccine Allocation

Vaccination is modelled as distribution of 5000 doses over 15 days from day 60 (333 doses per day). Vaccines are prioritized to the high risk group with 90% sensitivity, such that 4500 doses actually reach the high risk group, and 500 doses are given to the lower risk group. Figure A.1 illustrates vaccination coverage/counts by city/risk group for an example allocation of 80% to city A and 20% to city B.

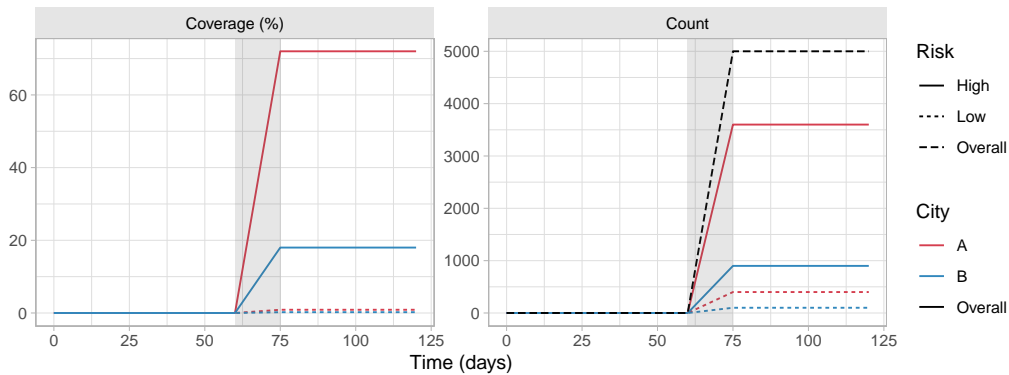
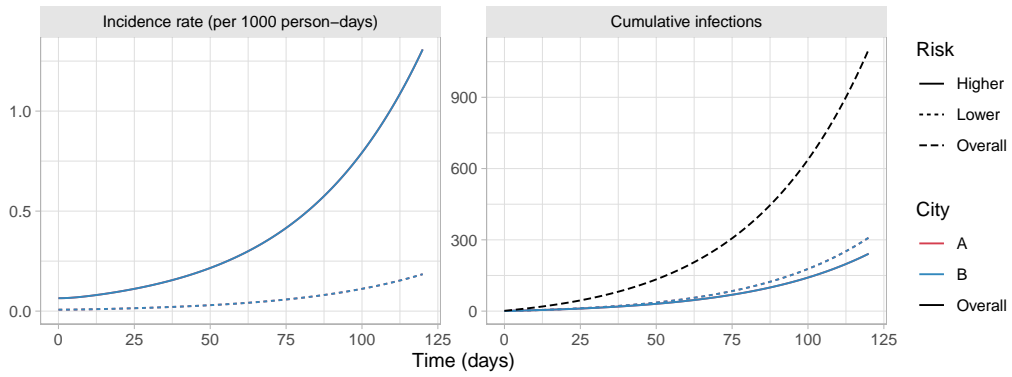


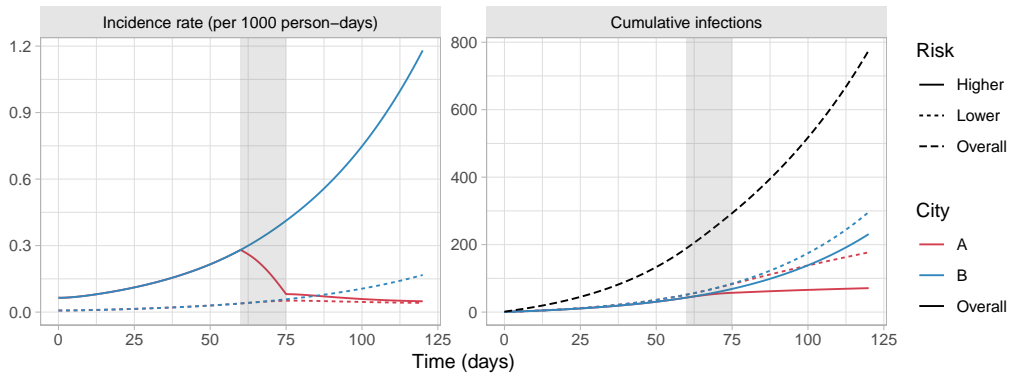
Figure A.1: Example vaccine allocation: 80% to city A, and 90% to high risk group

Gray bar indicates period of vaccine roll-out (days 60–75)

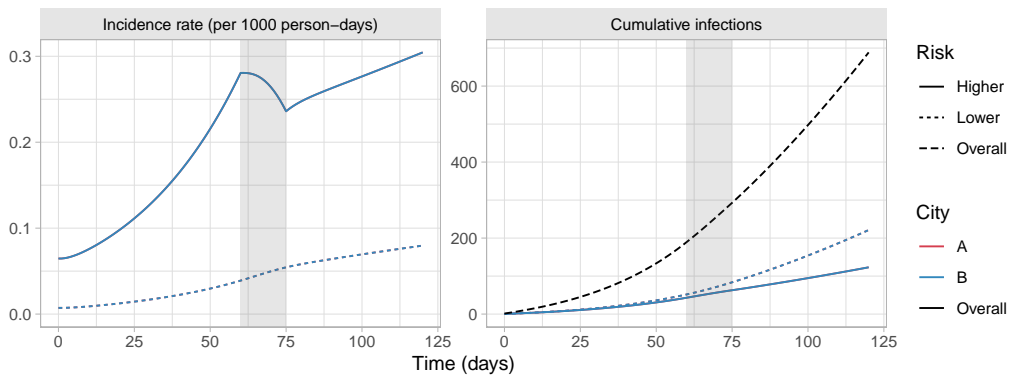
B Supplemental Results



(a) 100% city A



(b) 100% city A



(c) Optimal: 50% city A, 50% city B

Figure B.1: Modelled monkeypox incidence and cumulative infections in cities A and B with default parameters, under two different vaccine allocation scenarios

Gray bar indicates period of vaccine roll-out (days 60–75).

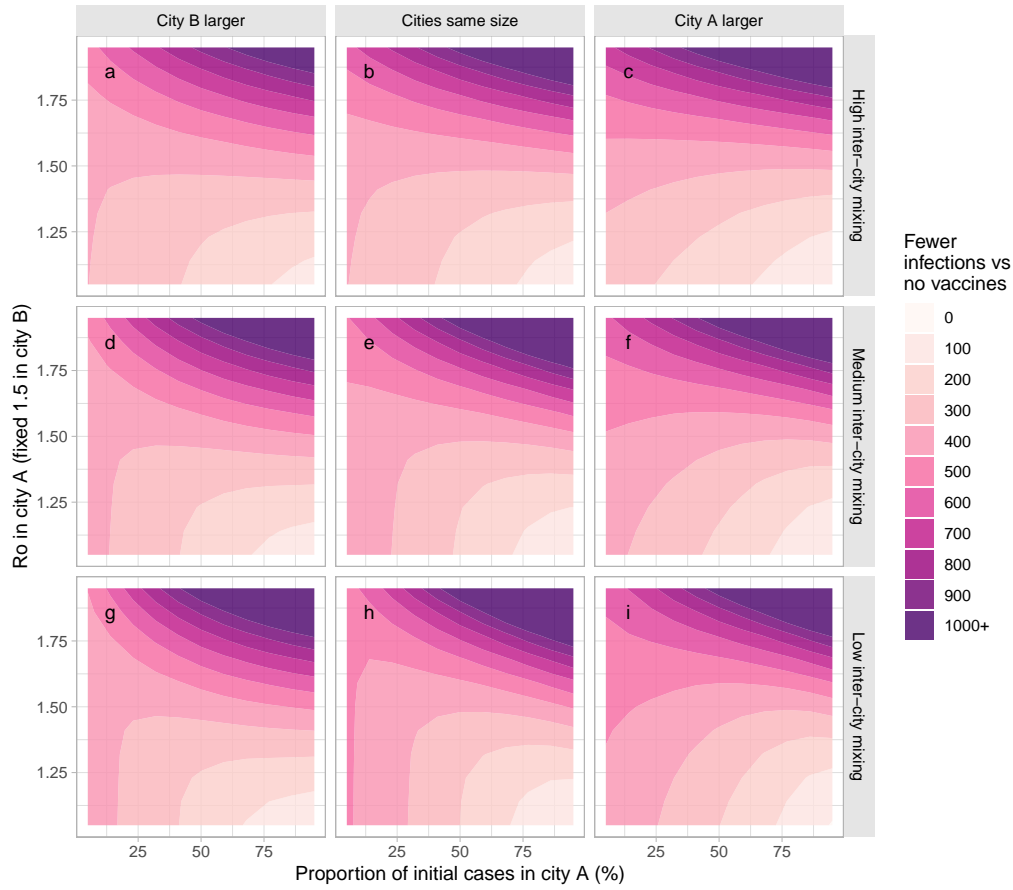


Figure B.2: Absolute fewer infections under optimal vaccine allocation versus no vaccination

R_0 in city A varies via the sexual activity among the high risk group in city A. Optimal allocation is defined as fewest cumulative infections by day 120. Larger city is 3 times the size of the other city. Most, moderate, and least inter-city mixing use $\epsilon_c = \{0.8, 0.9, 0.95\}$, respectively.

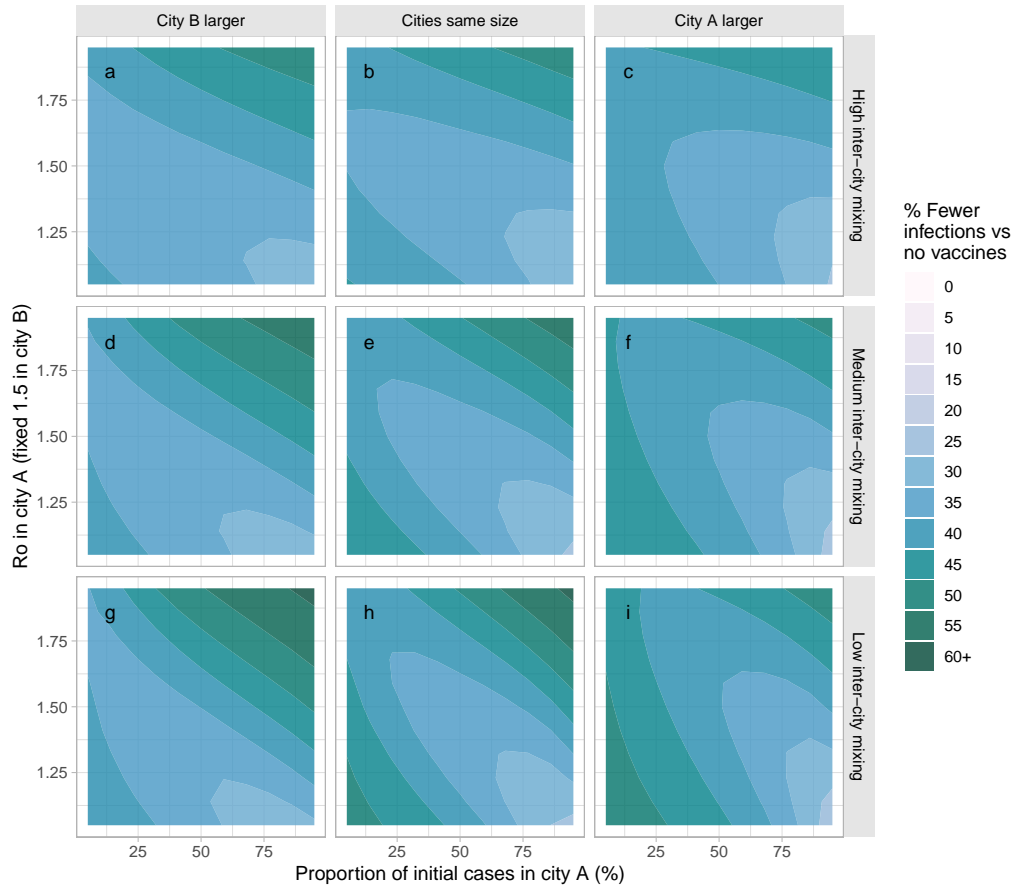


Figure B.3: Relative fewer infections under optimal vaccine allocation versus no vaccination

R_0 in city A varies via the sexual activity among the high risk group in city A. Optimal allocation is defined as fewest cumulative infections by day 120. Larger city is 3 times the size of the other city. Most, moderate, and least inter-city mixing use $\epsilon_c = \{0.8, 0.9, 0.95\}$, respectively.

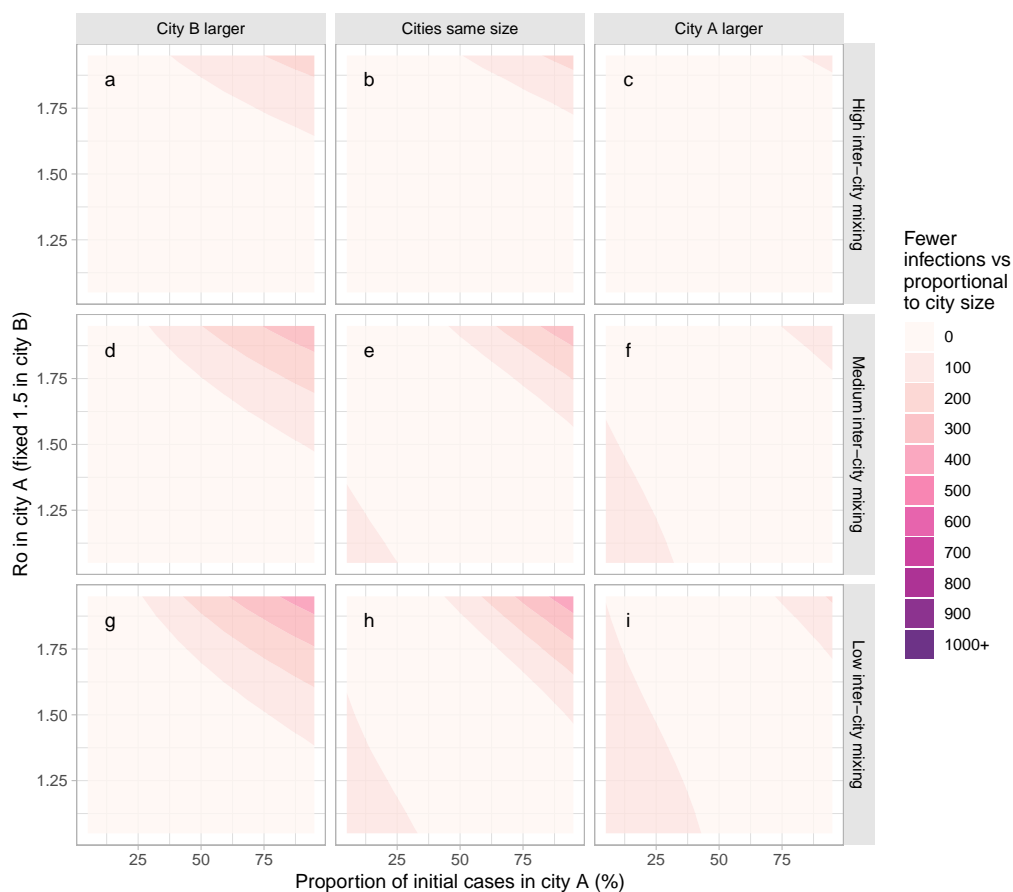


Figure B.4: Absolute fewer infections under optimal vaccine allocation versus allocation proportional to city size

R_0 in city A varies via the sexual activity among the high risk group in city A. Optimal allocation is defined as fewest cumulative infections by day 120. Larger city is 3 times the size of the other city. Most, moderate, and least inter-city mixing use $\epsilon_c = \{0.8, 0.9, 0.95\}$, respectively.

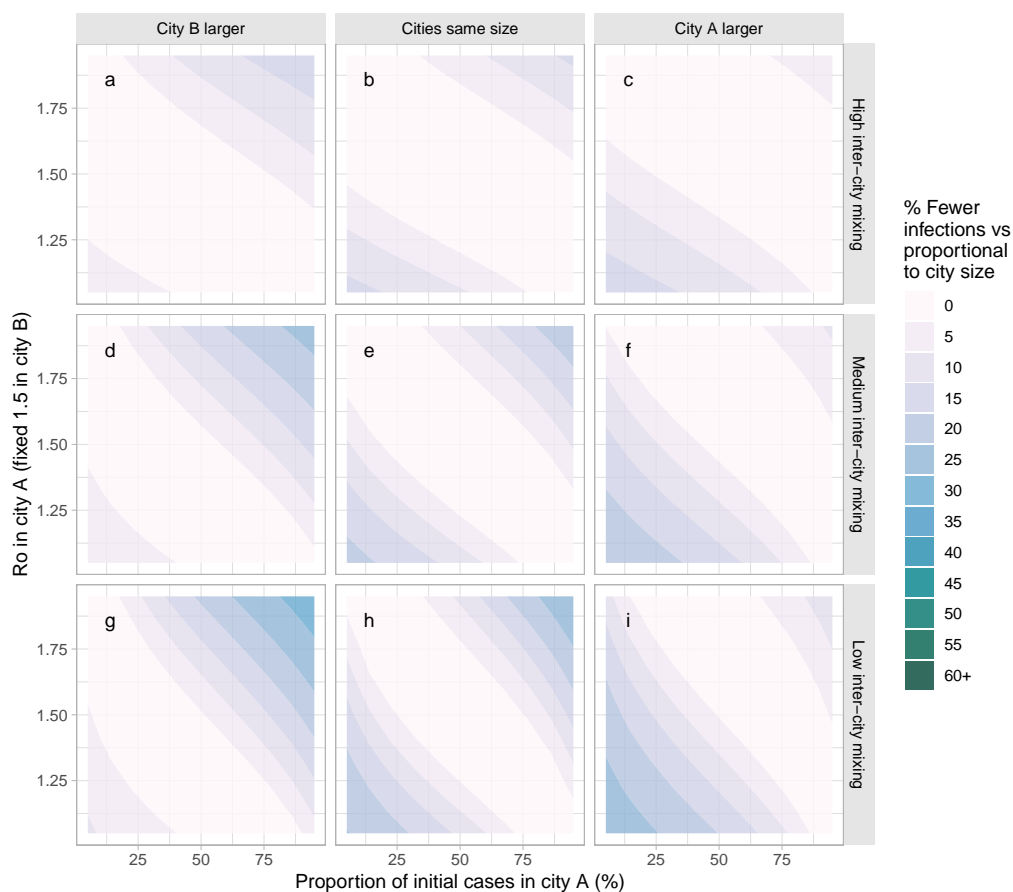


Figure B.5: Relative fewer infections under optimal vaccine allocation versus allocation proportional to city size

R_0 in city A varies via the sexual activity among the high risk group in city A. Optimal allocation is defined as fewest cumulative infections by day 120. Larger city is 3 times the size of the other city. Most, moderate, and least inter-city mixing use $\epsilon_c = \{0.8, 0.9, 0.95\}$, respectively.

References

- [1] A. Nold. "Heterogeneity in disease-transmission modeling". In: *Mathematical Biosciences* 52.3-4 (Dec. 1980), pp. 227–240.
- [2] G. P. Garnett and R. M. Anderson. "Balancing sexual partnerships in an age and activity stratified model of HIV transmission in heterosexual populations". In: *Mathematical Medicine and Biology* 11.3 (Jan. 1994), pp. 161–192.
- [3] O. Diekmann, J. A. Heesterbeek, and J. A. Metz. "On the definition and the computation of the basic reproduction ratio R_0 in models for infectious diseases in heterogeneous populations". In: *Journal of Mathematical Biology* 28.4 (1990), pp. 365–382.